Lymph Drainage during Wound Healing in a Hindlimb Lymphedema Mouse Model

Title page

Full title: Lymph drainage during wound healing in a hindlimb lymphedema mouse model

Running title: Lymph drainage and the wound healing process

Yukari Nakajima, RN, MS[1]; Emi Komatsu, RN, MS[2]; Kanae Mukai, RN, PhD[3]; Tamae Urai1, RN, MS[1]; Kimi Asano, RN, MS[4]; Mayumi Okuwa, RN, PhD[3]; Junko Sugama, RN, PhD[3]; Toshio Nakatani, MD, PhD[3]

(Yukari Nakajima and Emi Komatsu contributed equally to this research as first authors.)

1. Graduate School of Medical Sciences, Division of Health Science, Graduate Course of Nursing Science, Kanazawa University, Ishikawa Prefecture, Japan

2. Division of Nursing, Nagoya University Hospital

3. Institute of Medical, Pharmaceutical and Health Sciences; Kanazawa University; Ishikawa Prefecture; Japan

4. School of Nursing, Kanazawa Medical University, Ishikawa Prefecture, Japan

Address correspondence to:

Professor Toshio Nakatani, PhD,

Department of Clinical Nursing,

Graduate Course of Nursing Science,

Division of Health Sciences,

Graduate School of Medical Science,

Kanazawa University,

5-11-80 Kodatsuno, Kanazawa 920-0942, Japan

Tel: +81 76 265 2542

Fax: +81 76 234 4363

E-mail: nakatosi@staff.kanazawa-u.ac.jp

Abstract

Background: Although lymphedematous skin exhibits delayed wound healing, little is known about lymph drainage during wound healing. We investigated the wound healing process in the presence of lymphatic dysfunction.

Methods and Results: The right inguinal lymph nodes (iLN) and the surrounding tissue were excised in each mouse (on the operation side), and a sham operation was performed in the left hindlimb (the control side). The next day, full-thickness wounds were made on both hindlimbs. The right hindlimb exhibited acute edema until day 3; however, it started to improve after day 4, and the wound area and epithelialization ratio were similar on both sides. Indocyanine green (ICG) was injected into both hindlimbs to observe lymph flow. On the operation side, ICG leaked out of the surgical site or remained at the injection site until day 2. Some lymph flow towards the iLN was seen on day 3, and on day 10 lymph flow towards the axial LN (aLN) was detected on the operation side in all mice. On the operation side, the number of dermal lymph vessels was significantly increased on days 3 and 15. The dermal lymph vessel area of the peripheral wound was significantly smaller on the operation side.

Conclusions: In a hindlimb lymphedema mouse model, lymph transiently accumulated in subcutaneous tissue, before being gradually absorbed by the existing lymph vessels. The increase in the number of lymph vessels contributes to lymph drainage during wound healing. Acute lymphedema because of transient lymphatic dysfunction has little effect on wound healing.

(not more than 250 words: 250 words)

Introduction

The lymphatic system performs a crucial function by transporting protein-rich fluid from tissue back to the circulating blood through the lymphatico-venous junctions. Interstitial fluid, which is collected by the initial lymphatic capillary plexus, is transported by pre-collector lymphatic vessels to larger collecting lymphatic vessels and returned to the circulation through the thoracic duct. Lymphatic capillaries are present in the skin (mainly in the dermis) and most internal organs.[1,2] Harrell et al.[3] subjected a mouse to lymph node (LN) mapping. In their study, they reported that injection of Evans Blue dye the planta of the hindlimb labeled the popliteal LN, which drain centrally to the iliac and renal LN along the midline and also drain to the inguinal LN followed by the midline. After these injections, drainage from the inguinal LN (iLN) to the axillary LN (aLN) was only occasionally observed. In our preliminary experiment, the injection of patent blue violet into the outer surface of the hindlimb labeled the iLN, aLN, and the abdominal lymph vessels connecting these LN (data not shown).

Lymph vessels also play important roles in the pathogenesis of several diseases, such as cancer, various inflammatory conditions, and lymphedema. Lymph vessel impairment caused by surgery or radiotherapy can lead to secondary lymphedema. Lymphedema is a progressive disease characterized by gross swelling of the affected limb, accompanied by fibrosis,[2] decreased coordination and mobility, and susceptibility to infections.[4] Lymphedematous skin is so fragile that patients with lymphedema are recommended to perform various skin care procedures, such as keeping the skin clean, applying moisturizing cream, and examining their skin, in the clinical setting.[5] In addition, the skin of patients with lymphedema often exhibits repeated cellulitis and delayed wound healing due to its weakness; therefore, it is important to clarify the relationship between lymph drainage and wound healing in patients with lymphedema.

Generally, lymph vessels proliferate during inflammation.[6] After injuries, pro-inflammatory cytokines induce vascular endothelial growth factor (VEGF)-C messenger

RNA transcription, presumably through NF-kB-mediated promoter activation.[7] As a result, lymphatic regeneration starts at the peripheral edges of wounds.[8] Previous studies have reported that increased interleukin (IL)-6 or IL-10 expression prevented macrophage migration, resulting in delayed wound healing in a mouse tail lymphedema model.[9,10] Although these studies revealed that lymphedema leads to delayed wound healing associated with impaired immune responses, there have only been a few reports focusing on the relationship between lymph drainage function and wound healing. In our previous study,[11] we made full-thickness wounds on wild-type mice and investigated the role of lymph drainage in wound healing. As a result, it was found that the lymph vessels around the wound area expanded on days 1-3 after the wounding procedure, and these changes might have been due to the absorption of exudate leaking from the remaining blood vessels. This study suggested that the peripheral lymph vessels of wounds are more important for wound healing than those that form in granulation tissue. However, little is known about the drainage of lymph during wound healing in lymphedematous skin. Therefore, the aim of this study was to induce lymphedema in mice and evaluate the wound healing process and lymphatic dysfunction after surgery.

Materials and Methods

The experimental protocol and animal care procedures were in accordance with the Guidelines for the Care and Use of Laboratory Animals of Kanazawa University, Japan (AP-122521).

Animals

In total, 75 BALB/cCrSlc female mice (Sankyo Lab Service Corporation, Inc., Toyama, Japan) weighing 16.5-21.8 g were used. They were caged individually in an air conditioned room at a temperature of 25.0 ± 2.0°C, and the lights were kept on from 08:15 to 20:15 hours. Water and laboratory chow were given freely.

Mice hindlimb lymphedema model

We created a new mouse model of surgically-induced secondary lymphedema using a modified version of a previously published method.[12-16] The mice were anesthetized with a mixture of medetomidine (Nippon Zenyaku KogyoCo., Ltd., Fukushima, Japan), midazolam (Astellas Pharma Inc., Tokyo, Japan), and butorphanol (Meiji Seika Pharma Co., Ltd., Tokyo, Japan) (0.01 mg/g weight) via an intraperitoneal (IP) injection, and then the bodies of the mice were shaved completely, before hair removal cream was applied to the whole body. In our preliminary experiments, the iLN, aLN, and the abdominal lymph vessels connecting the iLN to the aLN were identified after the subcutaneous injection of 4 μl of 2% patent blue violet (Wako Pure chemical Industries, Ltd., Osaka, Japan) solution into the outer surface of the hindlimb. The iLN, aLN, and the abdominal lymph vessels connecting the iLN to the aLN were labeled on both sides in all mice. The right iLN were subsequently removed together with the associated peripheral lymph vessels and fat tissue using an electric knife, and then the surgical wounds were secured using 6-0 nylon simple interrupted sutures, before being bonded together and dressed with gauze (operation side). The left hindlimb was subjected to a sham operation, in which only the skin at 5 mm from the left iLN was excised so as to not injure the iLN (control side). After both operations, atipamezole (Nippon Zenyaku Kogyo Co.,

Ltd., Fukushima, Japan) was intraperitoneally injected as an antagonistic drug.

Wounding

The day after the operation, the mice were anesthetized with 2% isoflurane (Wako Pure chemical Industries, Ltd., Osaka, Japan). Then, a circular (4 mm in diameter) full-thickness skin wound that included the panniculus muscle was made in each hindlimb with a biopsy punch (Kai Industries, Gifu, Japan), and the removed skin was weighed in order to evaluate the degree of edema.

The wounds made on the operation and control sides were covered with hydrocolloid dressing (Tegaderm; 3M Health Care, Tokyo, Japan) to maintain a moist environment. All mice were wrapped with sticky bandages. Elizabethan collars were used to prevent the mice from biting their wounds.

Observation of ICG lymphography

Indocyanine green (ICG) is an intravascular fluorescent dye that has been used in ophthalmology to visualize the retinal and choroid vasculature for more than 40 years.[17] In order to investigate the lymph vessels that transport hindlimb interstitial fluid, we injected 2 μl ICG (2.5 mg/ml) into the outside of the hindlimb and massaged the injection site using absorbent cotton wool to promote ICG absorbance. After the injection, fluorescent images of lymphatic drainage channels were obtained using an infrared camera system (pde-neo) (Hamamatsu Photonics, Shizuoka, Japan). Examinations of ICG flow were conducted on days 1, 2, 3, 6, and 10 after the wounding procedure. After detecting lymph flow, grayscale images of ICG flow were taken.

Macroscopic observations

The day on which the wounds were made was designated as day 0, and the wound healing process was examined on days 0, 3, 6, 9, 12, and 15 after the wounding procedure. We

assessed each wound for edema, infection, and necrotic tissue. The wound edges were traced on polypropylene sheets, and photographs were taken at each timepoint. The traces on the sheets were captured with a scanner and transferred to a personal computer using Adobe Photoshop Elements 7.0 (Adobe System Inc., Tokyo, Japan), and the area of each wound was calculated using the image analysis software Scion Image Beta 4.02 (Scion Corporation, Frederick, Maryland, USA). On day 3, the wounds on the operation side revealed marked edema, and the amounts of exudate being released from them was measured by calculating the hydrocolloid weight on day 3 minus the unused hydrocolloid weight in order to evaluate the degree of edema. The mice that were used for the examinations of wound healing were not used to study ICG flow.

Tissue processing

The mice were euthanized via the IP injection of a large dose of pentobarbital sodium (0.5 mg/g weight) on day 3 or 15 after the wounding procedure. The operative field or the sham operative field and the surrounding intact skin were harvested, stapled onto transparent plastic sheets to prevent the specimens contracting excessively, and fixed in 4% paraformaldehyde in 0.1 mol/L phosphate buffer (pH 7.4) for 18 hours. The specimens were then dehydrated in an alcohol series, cleaned in xylene, and embedded in paraffin to prepare 5-μm serial sections. The resultant sections were stained with hematoxylin-eosin (H-E) or immunohistologically stained with anti-lymphatic vessel endothelial hyaluronan receptor 1 (LYVE-1) antibody (RELIATech GmbH, Germany) to detect lymphatic endothelial cells. The antigen unmasking procedure was antigen-dependent, as detailed below.

Immunohistochemical staining

After deparaffinization and rehydration, antigen unmasking was accomplished by heating the sections in a water bath, before incubating them in sodium citrate buffer (10 mM sodium citrate, 0.01% Tween 20; pH 6.0) for 20 minutes at approximately 100°C. The sections were

then washed with phosphate-buffered saline, before being incubated with anti-mouse LYVE-1 rabbit polyclonal antibody (RELIATech GmbH, Wolfenbuettel, Germany) at a concentration of 1∶100 at 4°C overnight. To detect the primary antibodies, the sections were incubated with polyclonal pig anti-rabbit immunoglobulins/horseradish peroxidase (DakoCytomation, Glostrup, Denmark) at a concentration of 1:100 for 30 minutes at room temperature, before being incubated with the Dako liquid DAB+ substrate chromogen system (Dako North America, California, USA) (brown chromogen) for 5 minutes or until staining was detected at room temperature. Light hematoxylin counterstaining was applied for 1 minute to visualize the cell nuclei. Negative control sections were obtained by omitting each primary antibody.

Microscopic examination

We calculated the epithelialization ratio (%) as follows: the length of the new epithelium/the distance between the wound edges. In order to evaluate the lymph vessels, we counted the number of lymph vessels and calculated the area of the lymph vessels in the dermis during examinations performed with a light microscope at a magnification of x200. The density of lymphatic endothelial cells in the dermis (number/mm^2) was calculated as follows: the number of endothelial cells detected by LYVE-1 in the dermis/the area subjected to microscope observation, and the lymph vessel area of the dermis was defined as the sum total of the area of the lymph vessels in the dermis in the microscopically examined area/the number of lymph vessels. These calculations were conducted for 3 areas around each wound, and the number of lymph vessels and the lymph vessel area of the dermis are described as mean values. The intact skin of wild type mice was also evaluated using the same parameters.

Statistical analysis

Data are expressed as mean ± SD values and were analyzed using JMP ® 8.0.1 (SAS, USA) (ANOVA, multiple comparisons Tukey-Kramer). The differences were considered

significant at $p < 0.05$.

Results

Wound healing process according to macroscopic observations

On day 0 (1 day after the removal of the iLN), the mice were wounded using a punch biopsy, and the weight of skin removed by the punch biopsy was measured. The mean weight of the removed skin on the operation and control sides on day 0 was 4.6 ± 1.4 mg and 2.4 ± 0.8 mg, respectively (p=0.003). From days 0 to 3, all wound surfaces were wet because of the release of exudate, and the areas of all wounds expanded (Figure 1a). Necrotic tissue was observed on some wound surfaces; however, epithelial tissue had started to cover the wound edges by day 3. Although the wounds on the operation side looked larger than those on the control side during the inflammatory phase, the difference was not significant (Figures 1a and 1b). The mean amounts of exudate produced on the operation and control sides between days 0 and 3 were 62.0 ± 24.6 mg and 50.4 ± 27.9 mg, respectively (p=0.25). After the inflammatory phase, the areas of all wounds gradually decreased, and epithelialization had been completed in all wounds (at the macroscopic level) by day 12. By day 15, all of the wounds had healed and exhibited scars. The wound area ratio did not differ significantly between the control and operation sides until day 15.

ICG lymphography

By subcutaneously injecting ICG into the hindlimbs of mice, we were able to pre-operatively detect the iLN, axillary LN (aLN), and the abdominal lymph vessels connecting the iLN to the aLN in all mice (Figure 2a). Table 1 shows the lymph flow detected by ICG lymphography. The ICG injected on the operation side leaked out of the surgical site field or remained at the ICG injection site until day 2 (Figure 2b). On the operation side, lymph flow toward the aLN was detected in 3of 9 mice on day 3; however, lymph transiently accumulated in the subcutaneous tissue at the surgical site, before being absorbed by the existing lymph vessels (Figure 2c). On day 6, lymph flow toward the aLN was detected on the operation side in 6 of 9 mice, and on day 10 lymph flow toward the aLN was detected on

the operation side in all mice (Figures 2d and 2e). On the control side, lymph flows toward the aLN was detected in all mice throughout the observation period.

Microscopic examination of lymph vessels

Figure 1c shows the epithelialization ratio data obtained in this study. Some epithelial tissue had started to cover the wound edges on day 3, and the epithelialization was complete in all wounds by day 12. The epithelialization ratios of the control and operation sides did not differ significantly until day 15.

We used the anti-LYVE-1 antibody (LYVE-1 is a marker of lymphatic endothelial cells) to detect lymph vessels in the skin. We only observed a few lymph vessels in the subcutaneous tissue so we only evaluated the lymph vessels in the dermis. The operation or sham operation sites were located below and near to the wound areas so we considered that the number of lymph vessels and the lymph vessel area at the operation or sham operation site would provide information about the drainage of exudate from the wound. The number of lymph vessels in the dermis was markedly higher on the operation side than on the control side on day 3 (p=0.0065) (Figures 3a, 3c, and 3d), and this difference persisted until day 15 (p=0.0024). These numbers were twice as high as those seen on the control side and in the intact skin. However, the lymph vessel area of the dermis was smaller than those on the control side and the intact skin on day 3, and gradually increased until day 15 (Figures 3b, 3e, and 3f). On day 15, the lymph vessel area of the dermis was similar in both groups (Figure 3b).

Discussion

Hindlimb lymphedema mouse model

Many previous studies of lymphedema have used mouse tail lymphedema models.[9, 18-20] In this study, we wanted to evaluate the wound healing process in the presence of lymphedema, and lymph flow during wound healing so we chose a hindlimb lymphedema mouse model, in

which the iLN together with the associated peripheral lymph vessels and fat tissue were excised. Marked hindlimb edema was seen on the operation side, and the amount of exudate produced was significantly higher on the operation side than on the control side until day 3. In addition, in ICG-based examinations no lymph flow was detected in the abdominal or axial areas of the operation side until day 2. These findings revealed that the operation performed in this study resulted in caused lymph flow obstruction in the groin region, resulting in lymphedema. However, lymph flow toward the aLN was detected in some mice on day 3, and it was found that most of the ICG flowing from the iLN to the aLN transiently accumulated at the surgical site, before being absorbed by the existing lymph vessels. ICG flow on the operation side was detected in all mice by day 10. Some previous studies of chronic lymphedema demonstrated that surgery alone did not have a sustained effect on the condition.[21, 22] In this study, a hindlimb lymphedema model, in which the iLN together with the associated peripheral lymph vessels and fat tissue were excised, produced acute, but not chronic, edema.

Lymph drainage during the wound healing process

In this study, we investigated the wound healing process and lymphatic dysfunction using a hindlimb lymphedema mouse model. In our previous study[11], we produced full-thickness wounds in the dorsal skin of mice and investigated the relationships among exudate production, the wound area, angiogenesis, lymphangiogenesis, and re-epithelialization during wound healing. In the latter study, we found that there were few new lymphatic capillaries in the granulation tissue that had formed approximately 2 days after the wounding procedure. Lymphatic regeneration began at the peripheral edges of the wounds from days 1 to 3, and the number of lymph vessels in the granulation tissue peaked on day 11, whereas blood vessels were first seen in the granulation tissue around days 3 or 4, and the number of blood vessels peaked on day 7. Therefore, the observed reduction in the amount of exudate produced by the wound appears to be related to blood vessel formation, rather than lymph vessel formation. In

this study, the number of lymph vessels on the control side was similar to that seen in the intact skin; however, the lymph vessel area was significantly greater on the control side than on the operation side on day 3. These findings support those of our previous study and suggest that the expanded lymph vessels seen in the peripheral areas of the wound or existing lymph vessels play more important roles in exudate drainage than the new lymph vessels that arise in granulation tissue in non-edematous skin. In addition, the number of lymph vessels on the operation side was significantly increased on days 3 and 15; however, the lymph vessel area on the operation side was significantly lower than that on the control side on day 3. Therefore, the number of new lymph vessels in the dermis increased in the peripheral areas of the wounds in the lymphedematous skin, which might have contributed to wound drainage, and this might have led to a reduction in edema and equivalent wound healing to that seen in the control. However, the drainage routes from the dermis to the subcutaneous peripheral wound were unclear because few lymph vessels were seen in the subcutaneous tissue in the present study.

It has been shown that VEGF-C can promote lymphangiogenesis by activating VEGF receptor (VEGFR)-2 and VEGFR-3 on lymphatic endothelial cells, and excess VEGF-C has been found to have ameliorative effects on edema produced by lymphatic obstruction in experimental models.[1, 23, 24] However, it has recently been demonstrated that mouse tail edema can resolve even if capillary lymphangiogenesis is completely absent. In brief, this shows that the resolution of edema is not dependent on new lymphatic growth across the surgical obstruction, distal lymph fluid crosses the regenerating wound area interstitially, and the balance of interstitial forces might be more important than lymphangiogenesis for maintaining fluid drainage and tissue volume during acute lymphedema.[19] Edema resolution was also observed in the present study. Although no ICG flow was detected until day 2 after the wounding procedure, ICG transiently accumulated in the subcutaneous tissue at the surgical site and then was gradually absorbed by the existing lymph vessels. As a result, the lymphedema was resolved. Therefore, the present study supports the findings of our previous

study.

We suggest that wound healing is not delayed by hindlimb lymphedema because lymph drainage re-starts. However, unfortunately we could not identify the detailed dermal lymph drainage routes from the peripheral wound areas to intact lymph vessels because deep lymph flow cannot be detected by ICG, and there were few lymph vessels in the subcutaneous tissue so we wonder how wound exudate drains to existing lymph vessels or LN. In addition, the hindlimb edema resolved after day 4 in the present study; therefore, it will be necessary to develop a sustained lymphedema model to allow us to evaluate lymph drainage during wound healing. These are the limitations of this study, and we will investigate these issues in future.

Acknowledgments

This study was supported by JSPS KAKENHI (Grant Number 25293430 to T. Nakatani) and research funding from Kanazawa University.

Author Disclosure Statement

The authors declare that they have no competing financial interests. All of the authors were involved in the study design, data collection, data analysis, and the editorial process and approved the final version of the manuscript.

References

1) Alitalo K., Tammela T., Petrova T.V., Lymphangiogenesis in development and human disease. Nature. 2005; 438 (7070): 946-53

2) Tammela T., Saaristo A., Holopainen T., Lyytikkä J., Kotronen A., Pitkonen M., Abo-Ramadan U., Ylä-Herttuala S., Petrova T.V., Alitalo K., Therapeutic differentiation and maturation of lymphatic vessels after lymph node dissection and transplantation. Nat Med. 2007; 13(12): 1458-66

3) Harrell M.I., Iritani B.M., Ruddell A., Lymph node mapping in the mouse. J Immunol Methods. 2008; 332(1-2): 170-4

4) Moshiri M., Katz D.S., Boris M., Yung E., Using lymphoscintigraphy to evaluate suspected lymphedema of the extremities. AJR Am J Roentgenol. 2002; 178(2): 405-12

5) Kerchner K., Fleischer A., Yosipovitch G., Lower extremity lymphedema update: pathophysiology, diagnosis, and treatment guidelines. J Am Acad Dermatol. 2008; 59(2): 324-31

6) Pullinger B. D., Florey H. W., Proliferation of lymphatics in inflammation. The Journal of Pathology and Bacteriology. 1937;45(1): 157-70

7) Ristimäki A., Narko K., Enholm B., Joukov V., Alitalo K., Proinflammatory cytokines regulate expression of the lymphatic endothelial mitogen vascular endothelial growth factor-C. J Biol Chem. 1998; 273(14): 8413-8

8) Yan A., Avraham T., Zampell J.C., Aschen SZ., Mehrara B.J., Mechanisms of lymphatic regeneration after tissue transfer. PLoS ONE. 2011; 6(2): e17201

9) Kimura T., Sugaya M., Blauvelt A., Okochi H., Sato S., Delayed wound healing due to increased interleukin-10 expression in mice with lymphatic dysfunction. J Leukoc Biol. 2013; 94(1): 137-45

10) Sugaya M, Lymphatic dysfunction and skin immunity. Japanese Journal of Lymphology. 2015; 38(1): 19-22

11) Shimamura K., Nakatani T., Ueda A., Sugama J, Okuwa M., Relationship between

lymphangiogenesis and exudates during the wound-healing process of mouse skin full-thickness wound. Wound Repair Regen. 2009; 17(4): 598-605

12) Wang G.Y., Zhong S.Z., A model of experimental lymphedema in rats' limbs. Microsurgery. 1985; 6(4): 204-10

13) Chen H.C., Pribaz J.J., O'brien B.M., Knight K.R., Morrison W.A., Creation of distal canine limb lymphedema. Plast Reconstr Surg. 1989; 83(6): 1022-6

14) Kanter M.A., Slavin S.A., Kaplan W., An experimental model for chronic lymphedema. Plast Reconstr Surg. 1990; 85(4): 573-80

15) Yano M., An experimental Non-Radiation Lymphedema model. Plast Reconstr Surg. 1993; 13: 572-77.

16) Oashi K., Furukawa H., Oyama A., Funayama E., Hayashi T., Saito A, Yamamoto Y., A new model of acquired lymphedema in the mouse hind limb: a preliminary report. Ann Plast Surg. 2012; 69(5): 565-8

17) Flower R.W., Injection technique for indocyanine green and sodium fluorescein dye angiography of the eye. Invest Ophthalmol. 1973; 12(12): 881-95

18) Tabibiazar R., Cheung L., Han J., Swanson J., Beilhack A., An A., Dadras S.S., Rockson N., Joshi S., Wagner R., Rockson S.G., Inflammatory manifestations of experimental lymphatic insufficiency. PLoS Med. 2006; 3(7): e254

19) Ongstad E.L., Bouta E.M., Roberts J.E., Uzarski J.S., Gibbs S.E., Sabel M.S., Cimmino V.M., Roberts M.A., Goldman J., Lymphangiogenesis-independent resolution of experimental edema. Am J Physiol Heart Circ Physiol. 2010; 299(1): H46-54

20) Shimizu Y., Shibata R., Shintani S., Ishii M., Murohara T., Therapeutic lymphangiogenesis with implantation of adipose-derived regenerative cells. J Am Heart Assoc. 2012; 1(4): e000877

21) Park H.S., Jung I.M., Choi G.H., Hahn S., Yoo Y.S., Lee T., Modification of a rodent hindlimb model of secondary lymphedema: surgical radicality versus radiotherapeutic ablation. Biomed Res Int. 2013; 2013: 208912

22) Lee-donaldson L., Witte M.H., Bernas M., Witte C.L., Way D., Stea B., Refinement of a rodent model of peripheral lymphedema. Lymphology. 1999; 32(3): 111-7

23) Ikomi F., Kawai Y., Nakayama J., Ogiwara N., Sasaki K., Mizuno R., Ohhashi T., Critical roles of VEGF-C-VEGF receptor 3 in reconnection of the collecting lymph vessels in mice. Microcirculation. 2008; 15(7): 591-603

24) Pytowski B., Goldman J., Persaud K., Wu Y., Witte L., Hicklin D.J., Skobe M., Boardman K.C., Swartz M.A., Complete and specific inhibition of adult lymphatic regeneration by a novel VEGFR-3 neutralizing antibody. J Natl Cancer Inst. 2005; 97(1): 14-21

Figure legends

Figure 1. Macroscopic examination of wound healing

a: Wounds of 4 mm in diameter were inflicted, and the wound healing process was recorded photographically (bar, 5 mm). b: The wound area ratios observed at each time point are shown. The *p*-values for each timepoint are as follows: day 3: p=0.80, day 6: p=0.34, day 9: p=0.46, day 12: p=0.73, day 15: p=0.21. c: The epithelialization ratio data are shown. The *p*-values for each observation point are as follows: day 3: p=0.80, day 6: p=0.43, day 9: p=0.79. Data are expressed as mean ± SD values. n=10 in each group (ANOVA, Tukey-Kramer).

Figure 2. The lymph flow detected on the operation side using ICG lymphography

The yellow arrows indicate lymph vessels, and the green arrow indicates the ICG injection site (hindlimb). a: The yellow “a” indicates the iLN detected before the operation. b: Lymph flow spread around the surgical site and remained in the subcutaneous tissue on day 2. c: ICG was still seen in the subcutaneous tissue and was then absorbed by the existing lymph vessels on days 3 and 6 (d). e: Lymph flow toward the aLN was detected in all mice on day 10.

Figure 3.

a: The number of lymph vessels in the dermis

The number of lymph vessels per mm^2 is shown in box graphs. Significant differences were detected between the operation and control sides or the intact skin on days 3 and 15 (operation versus intact skin: day 3: p=0.016, day 15: p=0.0062; operation versus control: day 3: p=0.0065, day 15: p=0.0024).

b: The lymph vessel area of the dermis

Significant differences were detected between the operation and control sides or the intact skin on day 3 (operation versus intact skin: p=0.0018; control versus intact skin: day 3: p=0.0437). Data are expressed as mean ± SD values, n=4-5 for each group, ANOVA, t-test, or

Tukey-Kramer *P <0.05, **P <0.01; c: Lymph vessels (arrows) stained with anti-LYVE-1 antibody on the operation side on day 3; d: Lymph vessels (arrows) stained with anti-LYVE-1 antibody on the control side on day 3; e: Lymph vessels (arrows) stained with anti-LYVE-1 antibody on the operation side on day 15; f: Lymph vessels (arrows) stained with anti-LYVE-1 antibody on the control side on day 15; bar, 50 μm

Figure 1

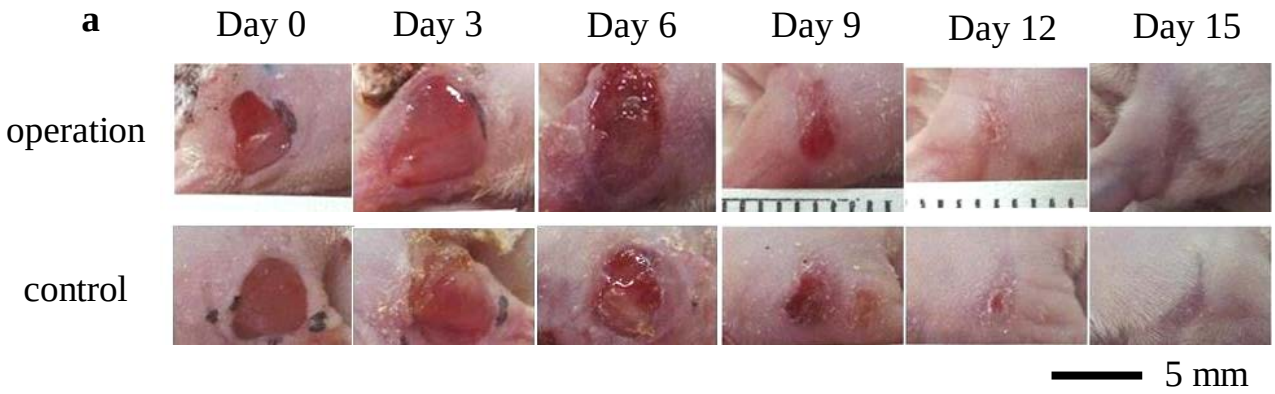
a
Day 0
Day 3
Day 6
Day 9
Day 12
Day 15
operation
control
5 mm

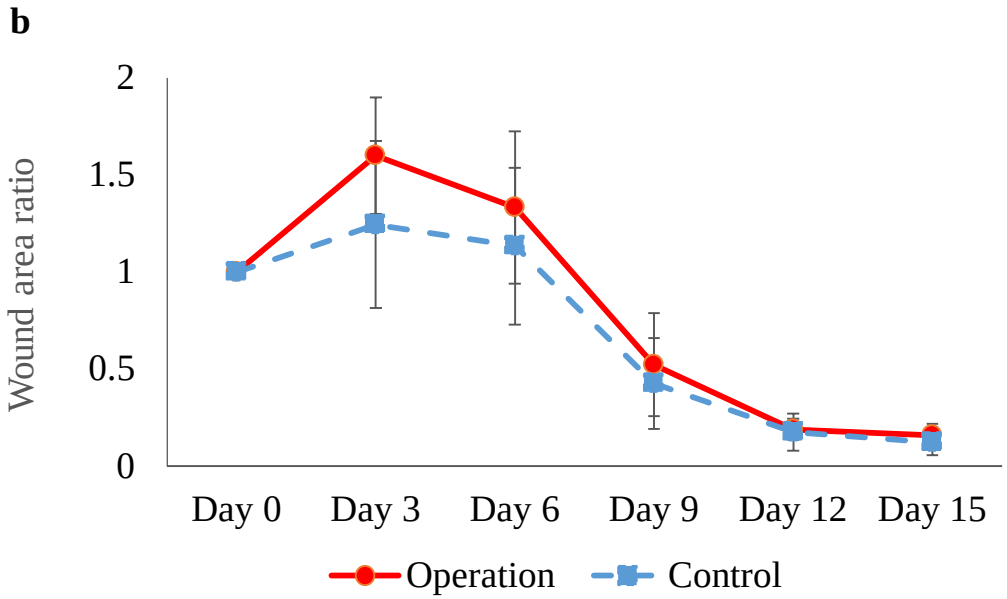
b
Wound area ratio
2
1.5
1
0.5
0
Day 0
Day 3
Day 6
Day 9
Day 12
Day 15
Operation
Control

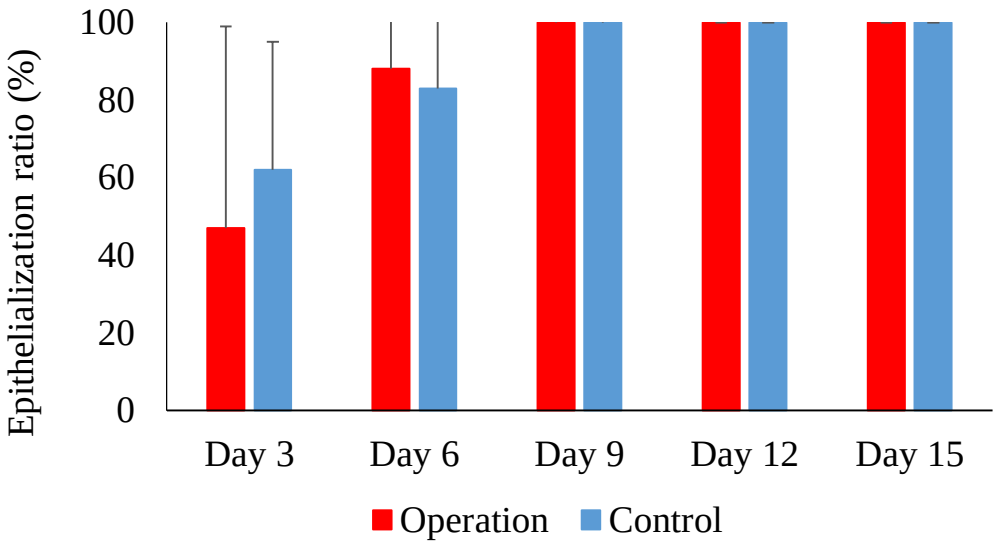
c
Epithelialization ratio (%)
100
80
60
40
20
0
Day 3
Day 6
Day 9
Day 12
Day 15
Operation
Control

Figure 2

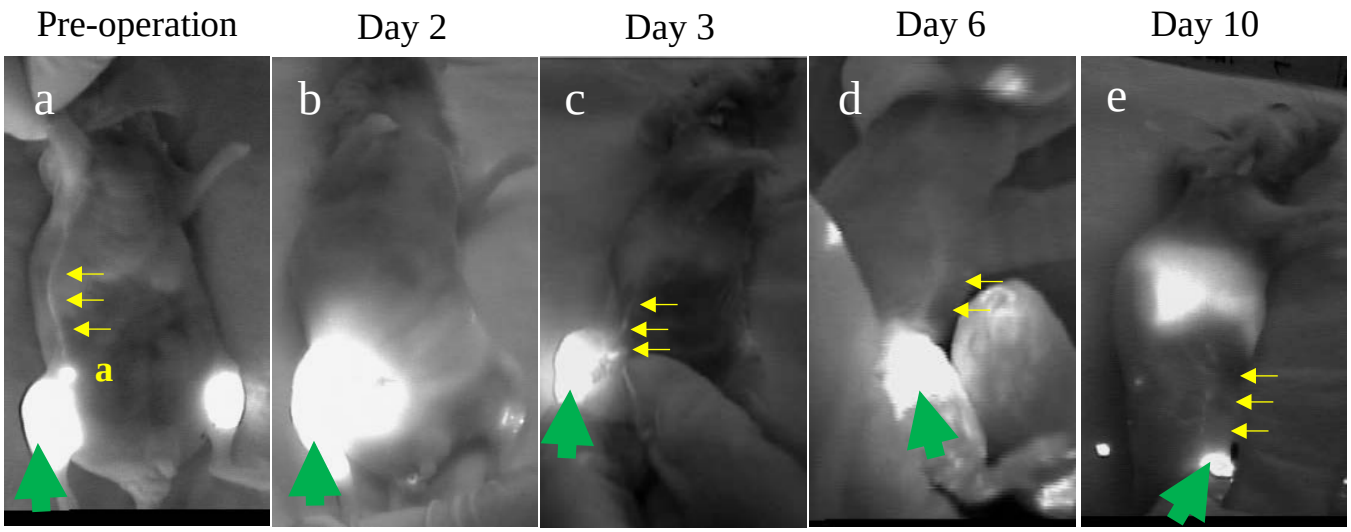

Figure 3

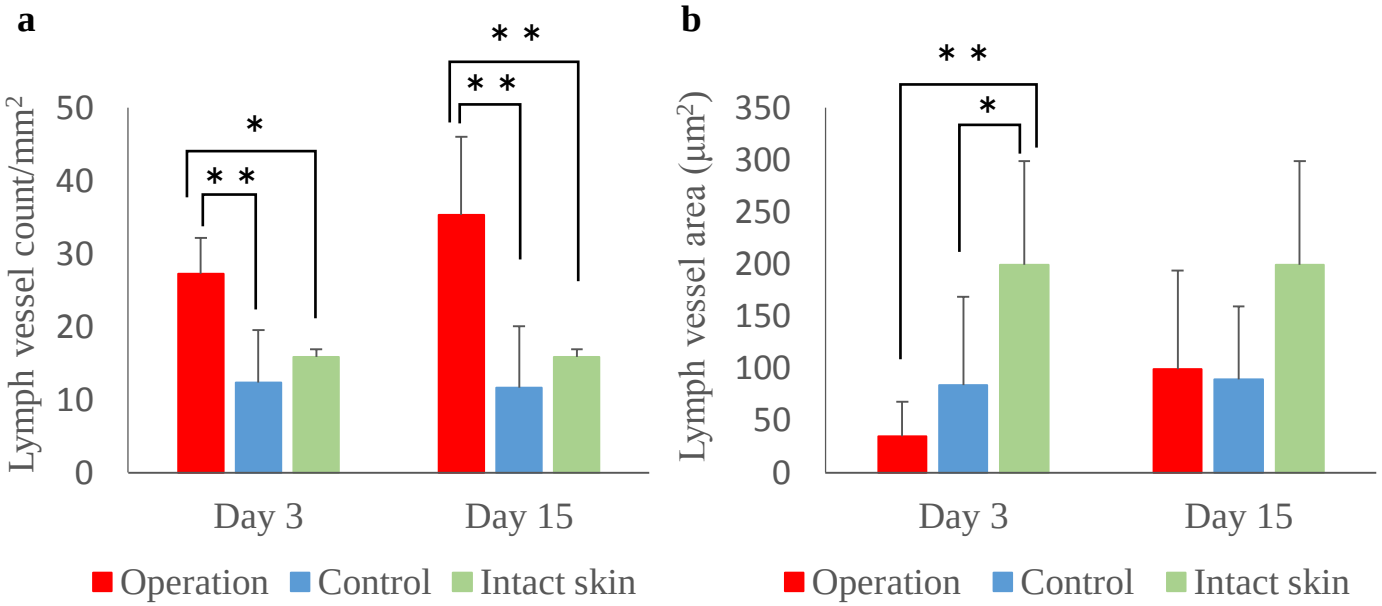
a
Lymph vessel count/mm2
50
40
30
20
10
0
*
* *
* *
* *
Day 3
Day 15
Operation
Control
Intact skin
b
Lymph vessel area (μm2)
350
300
250
200
150
100
50
0
* *
*
Day 3
Day 15
Operation
Control
Intact skin

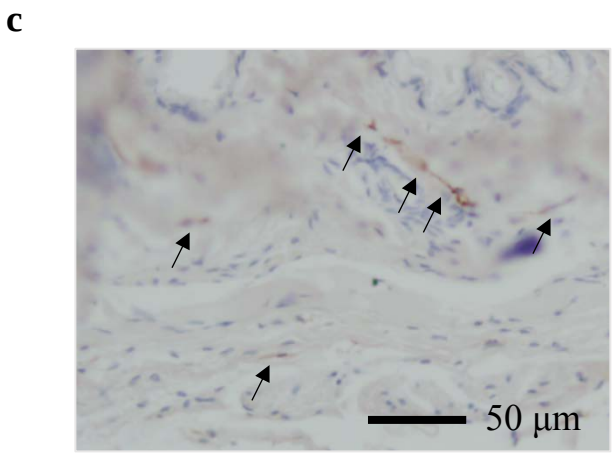
c
50 μm

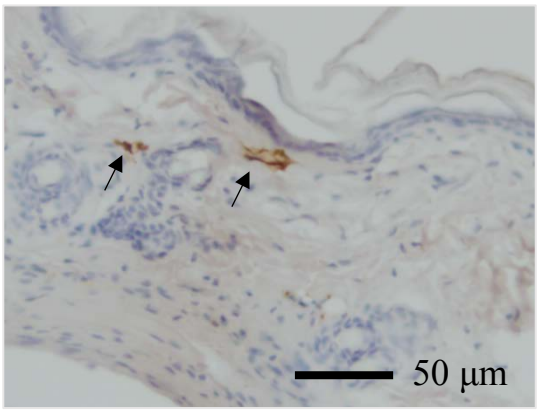
d
50 μm

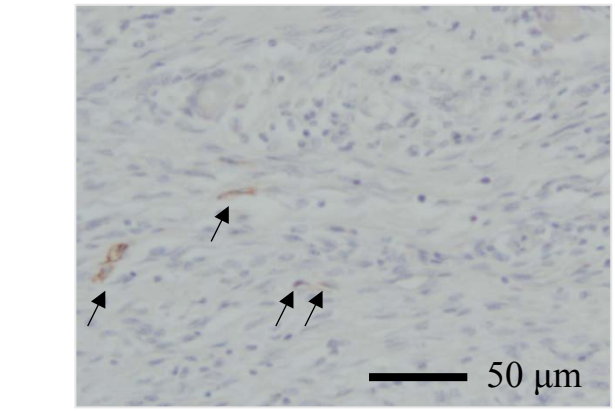
e
50 μm

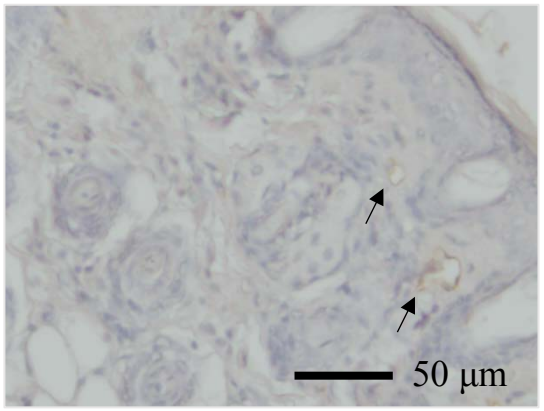
f
50 μm

Table 1. The number of mice in which lymph flow towards existing lymph vessels was detected by ICG lymphography

	After operation	Day 1	Day 2	Day 3	Day 6	Day 10
operation	0/5	0/5	0/5	3/9	6/9	5/5
control	5/5	5/5	5/5	5/5	5/5	5/5

The figures on the right indicate the total number of mice. The figures on the left indicate the number of mice in which lymph flow towards existing lymph vessels outside of the surgical site was detected. On day 10, lymph flow outside of the surgical site was detected in all mice.